

1 Dear Samuele Segoni,

2
3 Thank you very much for everything you have done for us about our manuscript entitled “**Rainfall threshold calculation for debris flow early warning in areas with scarcity of data**” (No.nhess-2017-333). We truly appreciate all of the thoughtful comments from you and the Referee, and we have now revised our manuscript accordingly with a list of changes detailed below.

8
9 **Response to Referee 1#:**

10
11 *In general, all the arisen questions have been fulfilled. On my view, the choice of proxies could be not fully agreeable. About item 18), I confirm that, on my view, rainfall intensity should be reported on x-axis in terms of cumulative values over time unit (also if for 1 hour time reference, the values are the same). Moreover the readability of x-axis in Graphs forming Figure 13 could be improved; for example, reporting only hours and putting date as x-label.*

12
13
14
15
16
17
18 Thanks a lot for your suggestions and advices, and we fully considered your advices and redrew the figures in Figure 13.

19
20
21 **Response to Editor:**

22
23 *1) I agree with the reviewer that the methodology has some major weaknesses. The choice of calculating API using 20 days is subjective and arbitrary. Why 20 and not 21, 30, 15, 10 or 5? Moreover, in several parts of the manuscript you state that in the literature other parameters are more frequently and conveniently used for debris flow modelling. Indeed, an overwhelming literature demonstrated that in similar cases of study I-D thresholds are more appropriate than thresholds accounting for antecedent rainfall conditions.*

24
25
26
27
28
29
30 Thank you very much for your kindly advices on this problem of this manuscript. As you suggested, firstly, we made 4 versions of the counting days when calculate API, 3days, 10days, 20days and 30days. The comparison among all the versions is shown in Table 6 (Line 469). It indicates that the value of the effective antecedent precipitations (P_{a0}) were increasing from 3 days to 20 days, while with the time last to 30 days, the value of P_{a0} was barely changed anymore. Therefore, it can be considered that the effect of a rainfall event usually diminished in 20 days. Hence, the numbers of previous indirect rainfall days (n) is identified as 20. At the same time, we analyzed the trend of the trigger rainfall of debris flow events in Guojuanyan gully, and made a debris flow triggering thresholds for the gully (Line 485, Figure 14). The comparison result shows that the laws of the two threshold curve are the same and validates that the calculated method of rainfall threshold proposed in this work is reasonable. We also discussed this in the Discussions part of the manuscript(Line 488-497).

31
32
33
34
35
36
37
38
39
40
41
42
43
44 *2) Fig. 7 and lines 234-260. This part is troublesome. You actually say that some kind of data are better than the ones you are going to use, then you state that you will use the worst data. You need to change this part because it introduces a major weakness in your research. Moreover, I do not agree with your conclusions. Fig.7 clearly shows that DF initiation cannot be characterized us-*

49 *ing only rainfall intensity, even if different time spans are taken into account (10',*
50 *1h and 1d intensity). You can get to this conclusion by observing that many DF*
51 *are below the annual average values. This encourages you to use antecedent*
52 *rainfall... HOWEVER, THESE PLOTS WOULD BE MORE INFORMATIVE IF*
53 *YOU PLOT DURATION ON THE X AXYS, to get I-D thresholds as mentioned in*
54 *the former comment (1b).*

55 We rewrote the whole paragraph about figure 7 to try to make it concise and clearly.
56 As you suggested, the main conclusion of Fig.7 is that the trigger rainfall of the debris
57 flow events had decreased obviously after the earthquake.

58
59 *3) The section 4.2.1 should be moved into the materials and methods section.*

60 *API should be explained the first time you mention it.*

61 This part has been moved to the materials and methods part as section 3.2 (Line
62 301-339).

63
64 *4) In the discussion section, you should clearly state that the threshold cannot be*
65 *applied elsewhere: the proposed approach is based on a procedure that can be*
66 *exported elsewhere only if a site-specific calibration is needed to develop specif-*
67 *ic thresholds for other test sites.*

68 This has been highlighted (Line 494-497).

69
70 *5) Others:*

71 We have checked the whole manuscript thoroughly again. Some additional and im-
72 portant references have also been added.

73
74 We wish that with the above revisions made, our manuscript can now be accepted for
75 publication on *Nature Hazards and Earth System Sciences* soon. Please do not hesi-
76 tate to contact me if you have any additional questions or comments.

77
78 Looking forward to hearing from you.

79
80 Regards

81
82 JIANG Yuanjun

83

84 **Rainfall threshold calculation for debris flow early**
85 **warning in areas with scarcity of data**

86 **Hua-li Pan**^{1, 2}, **Yuan-jun Jiang**^{1, 2, ✉}, **Jun Wang**³, **Guo-qiang Ou**^{1, 2}

87 ✉ Corresponding author's e-mail: yuanjun.jiang.civil@gmail.com

88 ¹ Key Laboratory of Mountain Hazards and Earth Surface Process, Chinese Academy of Sciences, Chengdu
89 610041, China

90 ² Institute of Mountain Hazards and Environment, Chinese Academy of Sciences, Chengdu 610041, China

91 ³ Guangzhou Institute of Geography, Guangzhou 510070, China

92 **Abstract:** Debris flows are one of the natural disasters that frequently occur in mountain ar-
93 eas, usually accompanied by serious loss of lives and properties. One of the most used ap-
94 proaches to mitigate the risk associated to debris flows is the implementation of early warning
95 systems based on well calibrated rainfall thresholds. However, many mountainous areas have
96 little data regarding rainfall and hazards, especially in debris flow forming regions. Therefore,
97 the traditional statistical analysis method that determines the empirical relationship between
98 rainstorm and debris flow events cannot be effectively used to calculate reliable rainfall
99 thresholds in these areas. After the severe Wenchuan earthquake, there were plenty of dipos-
100 its deposited in the gullies which resulted in lots of debris flow events subsequently. The trig-
101 gering rainfall threshold has decreased obviously. To get a reliable and accurate rainfall
102 threshold and improve the accuracy of debris flow early warning, this paper developed a
103 quantitative method, which is suit for debris flow triggering mechanism in meizoseismal areas,
104 to identify rainfall threshold for debris flow early warning in areas with scarcity of data based
105 on the initiation mechanism of hydraulic-driven debris flow. First, we studied the characteris-
106 tics of the study area, including meteorology, hydrology, topography and physical characteris-
107 tics of the loose solid materials. Then, the rainfall threshold was calculated by the initiation
108 mechanism of the hydraulic debris flow. **The comparison with other models and with alter-**
109 **nate configurations demonstrates that the proposed rainfall threshold curve is a function of**

110 the antecedent precipitation index (*API*) and 1-h rainfall. To test the proposed method, we se-
111 lected the Guojuanyan gully, a typical debris flow valley that during the 2008-2013 period
112 experienced several debris flow events and that is located in the meizoseismal areas of Wen-
113 chuan earthquake, as a case study. The comparison with other threshold models and with
114 configurations shows that the selected approach is the most promising to be used as a starting
115 point for further studies on debris flow early warning systems in areas with scarcity of data.

116 **Keywords:** Debris flow; rainfall threshold curve; rainfall threshold; areas with scarcity of
117 data

118 **1 Introduction**

119 Debris flow is rapid, gravity-induced mass movement consisting of a mixture of water,
120 sediment, wood and anthropogenic debris that propagate along channels incised on mountain
121 slopes and onto debris fans (Gregoretti et al., 2016). It has been reported in over 70 countries
122 in the world and often causes severe economic losses and human casualties, seriously
123 retarding social and economic development (Imaizumi et al., 2006; Tecca and Genevois, 2009;
124 Dahal et al., 2009; Liu et al., 2010; Cui et al., 2011; McCoy et al., 2012; Degetto et al., 2015;
125 Tiranti and Deangeli, 2015; Hu et al., 2016). Rainfall is one of the main triggering factors of
126 debris flows and is the most active factor when debris flows occur, which also determines the
127 temporal and spatial distribution characteristics of the hazards. As one of the important and
128 effective means of non-engineering disaster mitigation, much attention has been paid to
129 debris flow early warning by researchers (Pan et al., 2013; Guo et al., 2013; Zhou et al., 2014;
130 Wei et al., 2017). For rainstorm triggered debris flows, the precipitation and intensity of rain-
131 fall are the decisive factors of debris flow initiation, and a reasonable rainfall threshold target
132 is essential to ensure the accuracy of debris flow early warning. However, if there are some
133 extreme events occurred, such as an earthquake, the rainfall threshold of debris flow may
134 change a lot. Tang et al. (2012) analyzed the critical rainfall of Beichuan city and found that
135 the cumulative rainfall triggering debris flow decreased by 14.8%-22.1% when compared with
136 the pre-earthquake period, and the critical hour rainfall decreased by 25.4%-31.6%. Chen et al.
137 (2013) analyzed the pre- and post-earthquake critical rainfall for debris flow of Xiaogangjian
138 gully and found that the critical rainfall for debris flow in 2011 was approximately 23% lower

139 than the value during the pre-earthquake period. Other researches, such as Chen et al. (2008)
140 and Shied et al. (2009) has reached similar conclusions that the post-earthquake critical
141 rainfall for debris flow is markedly lower than that of the pre-earthquake period. The
142 Guojuanyang gully, a small gully located in the meizoseismal areas of the big earthquake, has
143 no debris flows under the annual average rainfall before 2008, but it became a debris flow
144 gully after the earthquake under the same conditions, even the rainfall was smaller than the
145 annual average rainfall. These indicated that earthquakes have a big influence on debris flow
146 occurrence. The earthquake triggered many unstable slopes, collapses, and landslides, which
147 have served as the source material for debris flow and shallow landslide in the years after the
148 earthquake (Tang et al. 2009, 2012; Xu et al. 2012; Hu et al. 2014). Therefore, the rainfall
149 threshold of debris flow post-earthquake is an important and urgent issue to study for debris
150 flow early warning and mitigation.

151 As an important and effective means of disaster mitigation, debris flow early warning
152 have received much attention from researchers. The rainfall threshold is the core of the debris
153 flow early warning , on which have a great deal of researches yet (Cannon et al., 2008; Chen
154 and Huang 2010; Baum and Godt, 2010;Staley et al., 2013; Winter et al., 2013; Zhou and Tang,
155 2014; Segoni et al., 2015; Rosi et al 2015). Although the formation mechanism of debris flow
156 has been extensively studied, it is difficult to perform distributed physically based modeling
157 over large areas, mainly because the spatial variability of geotechnical parameters is very
158 difficult to assess (Tofani et al., 2017). Therefore, many researchers (Wilson and Joyko, 1997;
159 Campbell, 1975; Cheng et al., 1998) have had to determine the empirical relationship between
160 rainfall and debris flow events and to determine the rainfall threshold depending on the
161 combinations of rainfall parameters, such as antecedent rainfall, rainfall intensity, cumulative
162 rainfall, et al.. Takahashi (1978), Iverson (1989)and Cui (1991) predicted the formation of
163 debris flow based on studies of slope stability, hydrodynamic action and the influence of pore
164 water pressure on the formation process of debris flow. Caine (1980) first statistically
165 analyzed the empirical relationship between rainfall intensity and the duration of debris flows
166 and shallow landslides and proposed an exponential expression($I = 14.82D^{-0.39}$). Afterwards,
167 other researchers, such as Wieczorek (1987), Jison (1989), Hong et al. (2005), Dahal and
168 Hasegawa (2008), Guzzetti et al. (2008) and Saito et al. (2010), carried out further research

169 on the empirical relationship between rainfall intensity and the duration of debris flows,
170 established the empirical expression of rainfall intensity - duration ($I = D$) and proposed
171 debris flow prediction models. Although I-D is the most used approach, other rainfall
172 parameters have been considered as well for debris flow thresholds. Shied and Chen (1995)
173 established the critical condition of debris flow based on the relationship between cumulative
174 rainfall and rainfall intensity. Zhang (2014) developed a model for debris flow forecasting
175 based on the water-soil coupling mechanism at the watershed scale. In addition, some
176 researchers have highlighted the importance to find more robust hydrological bases to
177 empirical rainfall thresholds for landslide initiation (Bogaard et al., 2018; Canli et al., in
178 review; Segoni et al., 2018). When data are scarce, a robust validation of a threshold model
179 can be based on a quantitative comparison with alternate versions of the threshold
180 (Althuwaynee et al., 2015) or with thresholds calculated with completely different approaches
181 (Frattini et al., 2009; Lagomarsino et al., 2015). Zhenlei Wei et al. (2017) investigated a
182 rainfall threshold method for predicting the initiation of channelized debris flows in a small
183 catchment, using field measurements of rainfall and runoff data.

184 Overall, the studies on the rainfall threshold of debris flow can be summarized as two
185 methods: the demonstration method and the frequency calculated method. The
186 demonstration method employs statistical analysis of rainfall and debris flow data to study the
187 relationship between rainfall and debris flow events and to obtain the rainfall threshold curve
188 (Bai et al., 2008; Tian et al., 2008; Zhuang, et al., 2009). The I-D approaches would be this
189 kind of method. This method is relatively accurate, but it needs very rich, long-term rainfall
190 database and disaster information; therefore, it can be applied only to areas with a history of
191 long-term observations. The frequency calculated method, assuming that debris flow and
192 torrential rain have the same frequency, and thus, debris flow rainfall threshold can be
193 calculated based on the rainstorm frequency in the mountain towns where have abundant
194 rainfall data but lack of disaster data (Yao, 1988; Liang and Yao, 2008). Researchers have also
195 analyzed the relationship between debris flow occurrences and precipitation and soil moisture
196 content based on initial debris flow conditions (Hu and Wang, 2003). However, this approach
197 is rarely applied to the determination of debris flow rainfall thresholds because it needs series
198 of rainfall data. Pan et al. (2013) calculated the threshold rainfall for debris flow pre-warning

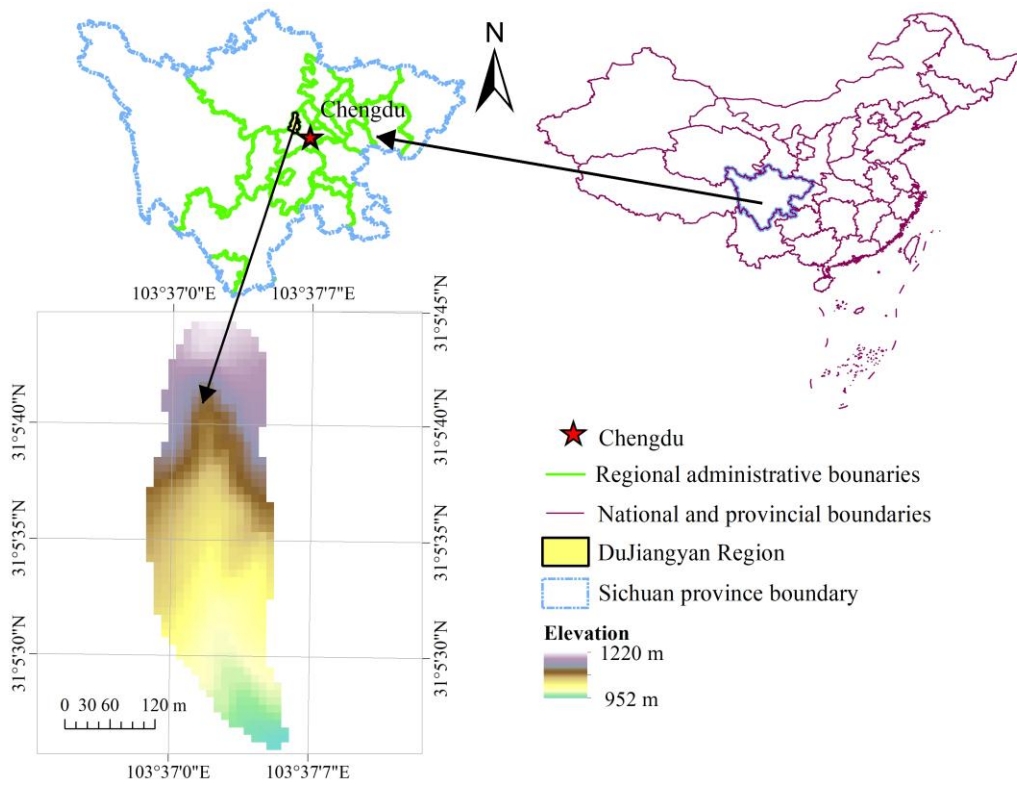
199 by calculating the critical depth of debrisflow initiation combined with the amount and
200 regulating factors of runoff generation.

201 Most mountainous areas have little data regarding rainfall and hazards, especially in
202 Western China. Neither the traditional demonstration method nor frequency calculated
203 method can satisfy the debris flow early warning requirements in these areas. Therefore, how
204 to calculate the rainfall threshold in these data-poor areas has become one of the most
205 important challenges for the debris flow early warning systems. To solve this problem, this
206 paper developed a quantitative method of calculating rainfall threshold for debris flow early
207 warning in areas with scarcity of data based on the initiation mechanism of hydraulic-driven
208 debris flows.

209 **2 Study site**

210 **2.1 Location and gully characteristics of the study area**

211 The Guojuanyan gully in Du Jiangyan city, located in the meizoseismal areas of the
212 Wenchuan earthquake, China, was selected as the study area (Fig. 1). It is located at the
213 Baisha River, which is the first tributary of the Minjiang River. The seismic intensity of the
214 study area was XI, which was the maximum seismic intensity of the Wenchuan earthquake.
215 The Shenxi Gully Earthquake Site Park is at the right side of this gully. The area extends from
216 $31^{\circ}05'27''$ N to $31^{\circ}05'46''$ N latitude and $103^{\circ}36'58''$ E to $103^{\circ}37'09''$ E longitude, covering an
217 area of 0.15 km² with a population of 20 inhabitants. The elevation range is from 943 m to
218 1222 m, the average gradient of the main channel is 270‰ (the average slope angle is 15.1°),
219 and the length of the main channel is approximately 580m.



220

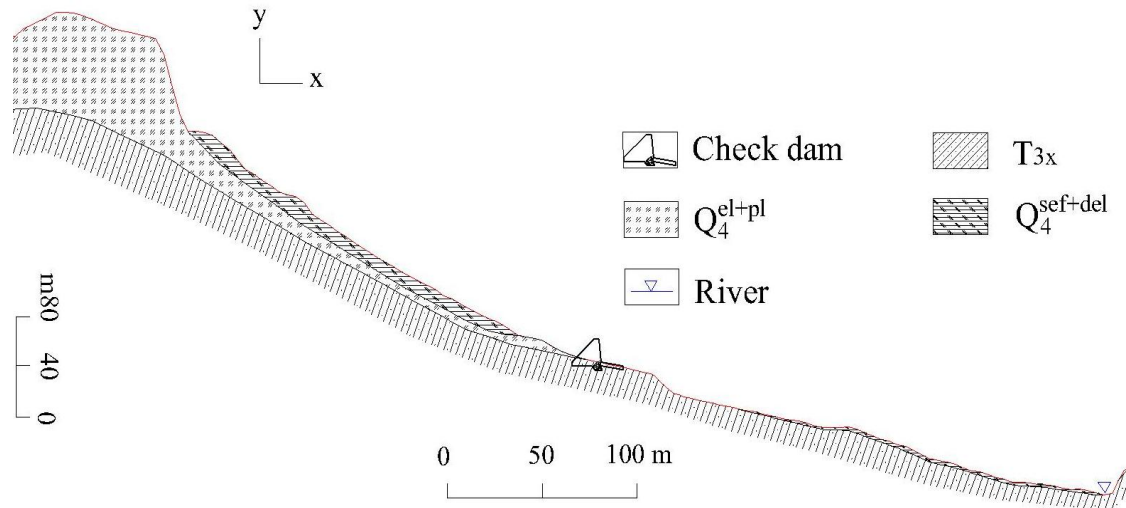
221

Figure 1. The location of the Guojuanyan gully

222

Geologically, the Guojuanyan gully is composed of bedrock and Quaternary strata. The bedrock is upper Triassic Xujiahe petrofabric (T_3x) whose lithology is mainly sandstone; mudstone; carbonaceous shale belonging to layered, massive structures; and semi solid-solid petrofabric. The Quaternary strata are alluvium (Q_4^{el+pl}), alluvial materials (Q_4^{pl+dl}), landslide accumulations and debris flow deposits ($Q_4^{sef+del}$). The thickness of the Quaternary strata ranges from 1 m to 20 m and varies greatly. The strata profile of the Guojuanyan gully is shown in Fig. 2.

228



229

230

Figure 2. The strata profile of the Guojuanyan gully (Jun Wang et al, 2017)

231

232

233

234

235

236

237

Geographically, the study area belongs to the Longmenshan Mountains. The famous Longmenshan tectonic belt has a significant effect on this region, especially the Hongkou-Yinxu fault. The study area has strong tectonic movement and strong erosion, and the main channel is “V”-shaped. The area is characterized by a rugged topography, and the main slope gradient interval of the gully is 20° to 40°, accounting for 52.38% of the entire study area.

Climatically, this area has a subtropical and humid climate, with an average annual temperature of 15.2°C and an average annual rainfall of 1200 mm (Wang et al., 2014).

238

2.2 Materials and debris flow characteristics of the study area

239

240

241

242

243

244

245

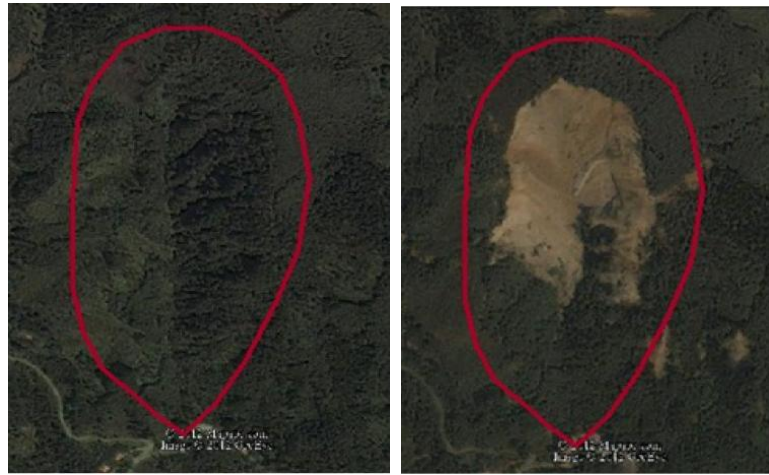
246

247

248

The Wenchuan earthquake generated a landslide in the Guojuanyan gully, leading to an abundance of loose deposits that have served as the source materials for debris flows. A comparison of the Guojuanyan gully before and after the Wenchuan earthquake is shown in Fig. 3. According to the field investigation and field tests, the landslide 3D characteristics induced by the earthquake and the infiltration characteristics of the loose materials are shown in Table 1 and Table 2 (Wang et al., 2016). They indicate that the volume of materials is more than $20 \times 10^4 \text{ m}^3$, and the infiltration capable of the earth surface have much increased. Therefore, the trigger rainfall for debris flow has decreased greatly. The Guojuanyan gully had no debris flows before the earthquake because of the lack of loose solid materials before the earthquake; however, it became a debris flow gully after the earthquake, and debris flows occurred in the

249 following years (Table 3). The specific conditions of these debris flow events were collected
 250 through field investigations and interviews. The field investigations and experiments deter-
 251 mined that the density of the debris flow was between 1.8 and 2.1 g/cm³. Unfortunately, there
 252 were no rainfall data before 2011, when we started field surveys in the Guojuanyan gully.



(a) 14 September, 2006 (b) 28 June, 2008

Figure 3. The Guojuanyan gully before (a) and after the Wenchuan earthquake (b) (from Google Earth)

Table 1. The landslide 3D characteristics induced by the earthquake in the study area

Average length /m	Average width /m	Average Height /m	Average depth /m	Slope /°	Volume /×10 ⁴ m ³
160	80	180	15	≅ 30	20

Table 2. The infiltration characteristics of solid materials in the study area

Infiltration curve	Infiltration rate	
	Initial infiltration /cm/min	Stable infiltration /cm/min
$f = 0.6529 \cdot \exp(-0.057 \cdot t)$	3.52	0.34

Table 3. The specific conditions of debris flow events in the Guojuanyan gully after the earthquake

Time	Volume (10 ⁴ m ³)	Surges	Rainfall data record
24 September, 2008	0.6	1	No
17 July, 2009	0.8	1	No
13 August, 2010	4.0	3	No
17 August, 2010	0.4	1	No
1 July, 2011	0.8	1	Yes
17 August, 2012	0.7	1	Yes
9 July, 2013	0.4	1	Yes
26 July, 2013	2.0	2	Yes
18 July, 2014	1.5	1	Yes

260 **2.3 Debris flow monitoring and streambed survey of the study area**

261 After the Wenchuan earthquake, continuous field surveillance was undertaken in the
262 study area. A debris flow monitoring system was also established in the study area. To identify
263 the debris flow events, this monitoring system recorded stream water depth, precipitation and
264 real-time video of the gully (Fig. 4). The water depth was measured using an ultrasonic level
265 meter, and precipitation was recorded by a self-registering rain gauge. The real-time video
266 was recorded onto a data logger and transmitted to the monitoring center, located in the In-
267 stitute of Mountain Hazards and Environment, Chinese Academy of Sciences. When a rain-
268 storm or a debris flow event occurs, the realtime data, including rainfall data, video record,
269 and water depth data, can be observed and queried directly in the remote client computer in
270 the monitoring center. Fig. 5 shows images taken from the recorded video. These data can be
271 used to analyze the rainfall or other characteristics, such as the 10-min, 1- and 24-h critical
272 rainfall. The recorded video is usually used to analyse the whole inundated process of debris
273 flow events and to identify debris flow events as well as the data from rainfall, flow depth, and
274 field investigation.



275 (a) Real-time camera and rain gauge (b) Ultrasonic level meters

277 **Figure 4.** Debris flow monitoring system in the study area



278

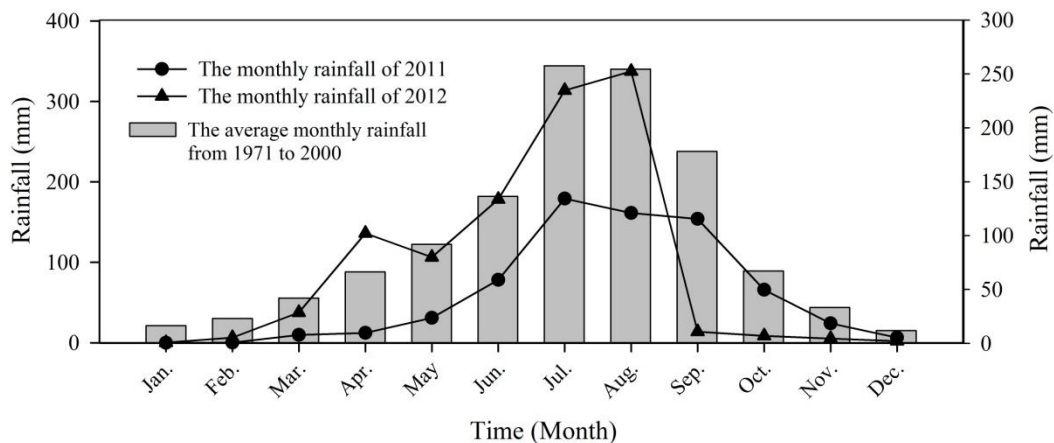
279

Figure 5. Real-time images from video taken during the debris flow movement

280 **2.4 Data collection and the characteristics of rainfall**

281 The Wenchuan earthquake occurred in the Longmenshan tectonic belt, located on the
 282 eastern edge of the Tibetan plateau, China, which is one of three rainstorm areas of Sichuan
 283 Province (Longmen mountain rainstorm area, Qingyi river rainstorm area and Daba moun-
 284 tain rainstorm area). Heavy rainstorms and extreme rainfall events occur frequently. Because
 285 there were few data in the mountain areas, we collected the rainfall data from 1971- 2000 and
 286 2011-2012 (from our own on-site monitoring); the characteristics of the rainfalls are as fol-
 287 lowing:

288 (1) Abundant precipitation: The average annual precipitation was 1177.3 mm from 1971 to
 289 2000, and the average monthly precipitation is shown in Fig. 6. From 1971 to 2000, the min-
 290 imum annual precipitation of 713.5 mm occurred in 1974, and the maximum annual precipi-
 291 tation of 1605.4 mm occurred in 1978. The total precipitation in 2012 is 1148mm, in the trend
 292 range of the historical data.



293

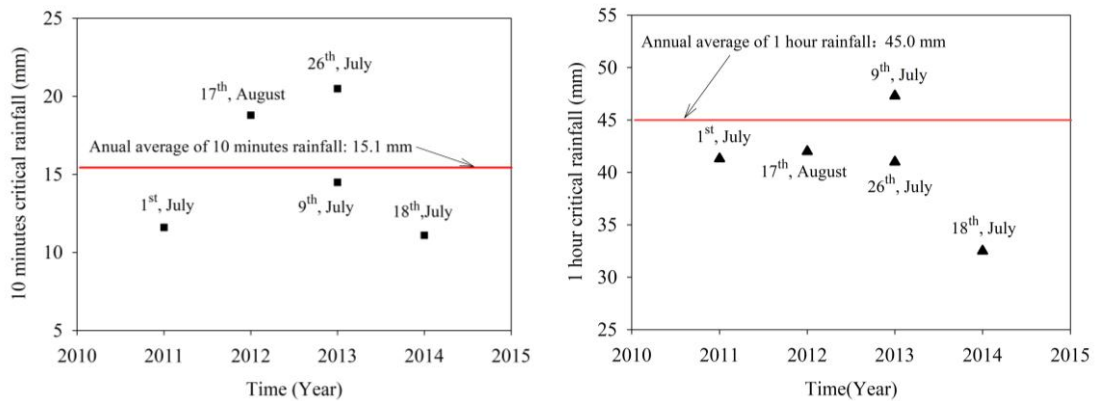
294 **Figure 6.** The average monthly precipitation of the Guojuanyan gully from 1971 to 2000 and the
 295 monthly rainfall of 2011 and 2012

296 (2) **Seasonality of the distribution of precipitation:** from Fig. 6 we can observe that rain-
 297 fall is seasonal, with approximately 80% of the total rainfall occurring during the monsoon
 298 season (from June to September) and the other 20% in other seasons. And the laws of
 299 monthly rainfall in 2011 and 2012 coincide to the historical data. For instance, in 2012, the

300 total annual rainfall in this area was approximately 1148 mm, and rainfall in the monsoon
 301 season from June to September was 961 mm, accounting for 83.7% of the annual total.

302 (3) The rainfall intensity has great differences. From 1971 to 2000, the maximum month-
 303 ly rainfall was 592.9 mm, the daily maximum rainfall was 233.8 mm, the hourly maximum
 304 rainfall was 83.9 mm, the 10 minute maximum rainfall was 28.3 mm, and the longest contin-
 305 uous rainfall time was 28 days.

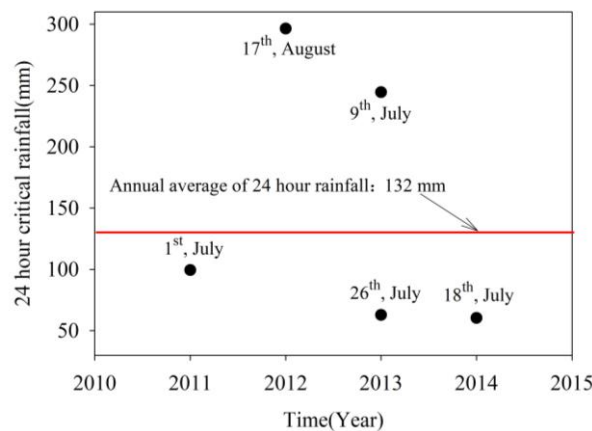
306 Debris flow field monitoring data and on-site investigation data were used to identify the
 307 debris flow events and to analyze the characteristics of the rainfall pattern and the critical
 308 rainfall characteristics. Analyzing the typical rainfall process curves (Fig. 13), we can find that
 309 the hourly rainfall pattern of the Guojuanyang gully is the peak pattern, displaying the single
 310 peak and multi-peak, a characteristic of short-duration rainstorms. Through the statistical
 311 analysis of the 10-min, 1-, and 24-h critical rainfall of debris flow events after the earthquake,
 312 their characteristics can be obtained, as shown in Fig. 7.



313

314

(a) The 10-min critical rainfall (b) The 1-h critical rainfall



315

316

(c) The 24-h critical rainfall

317

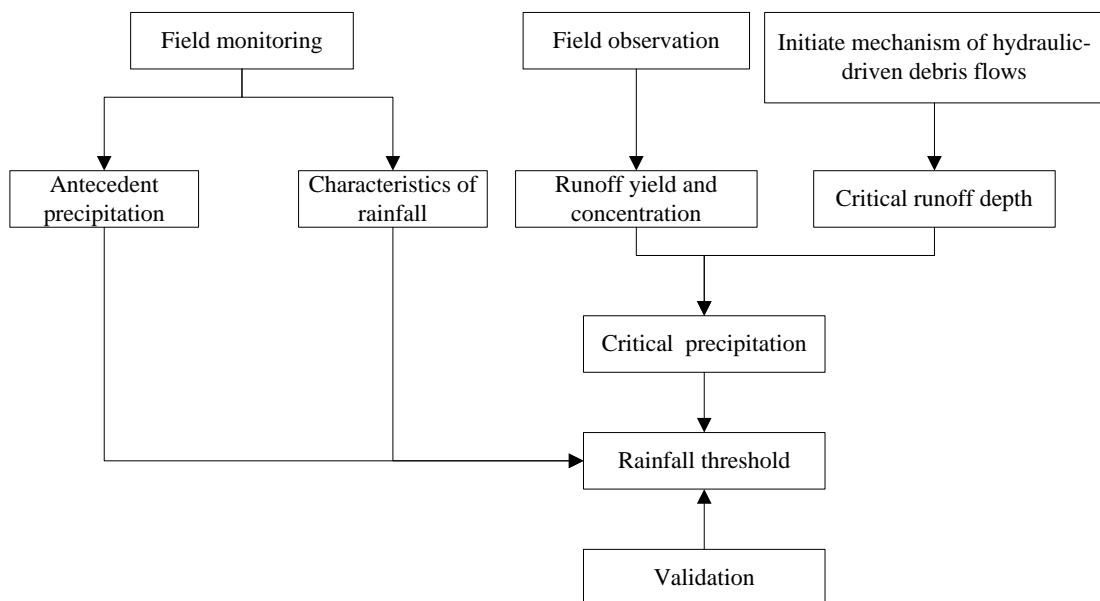
Figure 7. The critical rainfall of debris flows in the Guojuanyan gully

318 According to the Sichuan Hydrology Record Handbook (Sichuan Water and Power De-
 319 partment 1984), during 1940-1975, the annual average of maximum 10-min rainfall of the
 320 study area is approximately 15.1 mm, the maximum 1-h rainfall is 45.0 mm and the annual
 321 average of maximum 24-h rainfall is 132 mm. Fig. 7 shows that the majority of the debris flow
 322 events in 2011-2014 occurred in a rainfall below the annual average values. It convinced that
 323 the rainfall threshold of debris flow was decreased obviously after the earthquake.

324 3 Materials and methods

325 This study makes an attempt to analyze the trigger rainfall threshold for debris flow by
 326 using the initiation mechanism of debris flow. Firstly, to analyze the rainfall characteristics of
 327 the watershed by using the field monitoring data; then to calculate the runoff yield and con-
 328 centration progress based on field observation. Additionally, the critical runoff depth to initi-
 329 ate debris flow was calculated by the initiation mechanism with the underlying surface condi-
 330 tion (materials, longitudinal slope, etc.) of the gully. Then, the corresponding rainfall for the
 331 initiation of debris was back-calculated based on the stored- full runoff generation. At last,
 332 these factors were combined to build the rainfall threshold model. This method can be applied
 333 to the early warning system in the areas with scarcity of rainfall data.

334 The flow chart of the research is shown in Fig. 8.



335
 336

337

Figure 8. The flow chart of the research

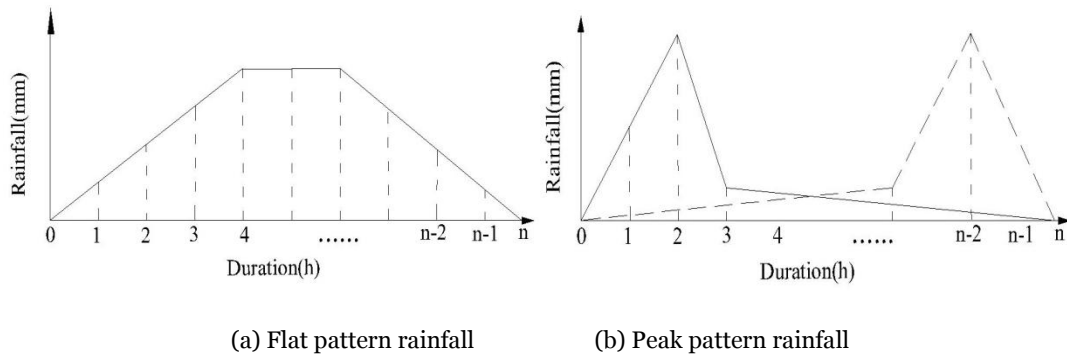
338 The main influence factors for the formation of debris flow event include three parts: a
339 steep slope of the gully (served as potential energy condition), abundant solid materials
340 (source condition) and water source condition (usually is rainfall condition for rainstorm
341 debris flow). For rainstorm debris flow events, the precipitation and intensity of rainfall are
342 the decisive factors of debris flow initiation. If there is no earthquakes or other extreme events,
343 the topography of the gully can be considered relatively stable. In contrast, rainfall conditions
344 and the distribution of solid materials that determine the occurrence of debris flows can
345 display temporal and spatial variation within the same watershed. Therefore, it is common to
346 provide warning of debris flows based rainfall data after assessing the supply and distribution
347 of loose solid materials. In Takahashi's model, the characteristics of soil, such as the porosity
348 and the hydraulic conductivity of soils, are not considered, and considered the characteristic
349 particle size and the volume concentration of sediment; while the characteristics of
350 topography is mainly represented by the longitudinal slope of the gully. Furthermore, in the
351 stored-full runoff model, the maximum storage capacity of watershed, which mainly decided
352 by the porosity and permeability of the soil, may represent the characteristic of the hydraulic
353 conductivity of solid material to a certain extent. Therefore, this study wouldn't consider the
354 hydraulic conductivity any more.

355 **3.1 Rainfall pattern and the spatial-temporal distribution characteristics**

356 Mountain hazards such as debris flows are closely related to rainfall duration, rainfall
357 amount and rainfall pattern (Liu et al., 2009). Rainfall pattern not only affects the formation
358 of surface runoff but also affects the formation and development of debris flows. Different
359 rainfall patterns result in different soil water contents; thus, the internal structure of the soil,
360 stress conditions, shear resistance, slip resistance and removable thickness can vary. The ini-
361 tiation of a debris flow is the result of both short-duration heavy rains and the antecedent
362 rainfall (Cui et al., 2007; Guo et al., 2013). Many previous observational data have shown that
363 the initiation of a debris flow often appears at a certain time that has a high correlation with
364 the rainfall pattern (Rianna et al., 2014; Mohamad Ayob Mohamadi, 2015).

365 The precipitation characteristics not only affect the formation of runoff, also affect the
366 formation and development of the debris flow. Different rainfalls result in different soil water
367 contents, and thus the internal structure of the soil, stress conditions, corrosion resistance

368 and slip resistance can vary (Pan et al., 2013). Based on the rainfall characteristics, rainfall
 369 patterns can be roughly divided into two kinds, the flat pattern and the peak pattern, as shown
 370 in Fig. 9. If the rainfall intensity has little variation, there is no obvious peak in the whole
 371 rainfall process; such rainfall can be described as flat pattern rainfall. **If the soils characterized**
 372 **by low hydraulic conductivity, this kind of rainfall can hardly trigger a debris flow separately,**
 373 **and the debris flows will mainly be triggered by the great amount of effective antecedent pre-**
 374 **cipitation.** While if the rainfall intensity increases suddenly during a certain period of time,
 375 the rainfall process will have an obvious peak and is termed peak pattern rainfall. If the hy-
 376 draulic conductivity is high enough, the rainfall can totally entering the soil and mass can
 377 move easily. These debris flows are mainly controlled by the short-duration heavy rains. Peak
 378 pattern rainfall may have one peak or multi-peak (Pan, et al., 2013).



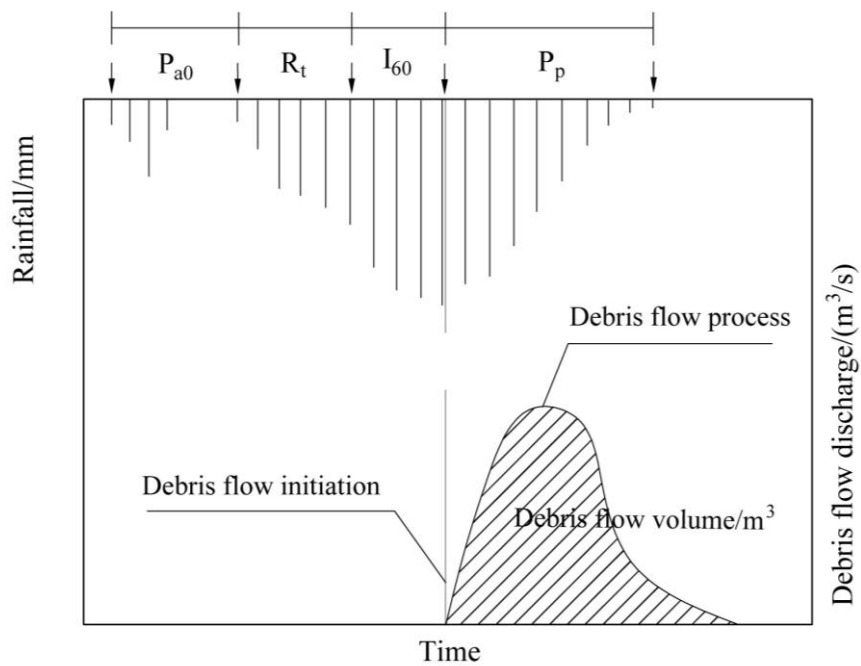
381 **Figure 9.** The diagram of rainfall patterns

382 Through analyzing the rainfall data of the Guojuanyan gully, the rainfall pattern and the
 383 spatial-temporal distribution characteristics can be obtained.

384 **3.2 The calculation of the antecedent precipitation index (API)**

385 The rainfall factor influencing debris flows consists of three parts: indirect antecedent
 386 precipitation (IAP) (it is P_{a0} in this paper), direct antecedent precipitation (DAP) (it is R_t in this
 387 paper), and triggering precipitation (TP) (it is I_{60} in this paper). The relationships among them
 388 are shown in Figure 10. Obviously, IAP increases soil moisture and decreases the soil stability,
 389 and DAP saturates soils and thus decrease the critical condition of debris flow occurrence.
 390 Although TP is believed to initiate debris flows directly, its contribution amounts to only 37%
 391 of total water (Cui et al. 2007). Guo et al (2013) analyzed the rainstorms and debris flow

392 events during June and September in 2006 and 2008, there were 208 days with antecedent
 393 rainfall more than 10mm, approximately 57% days of the rain season. Among them, there
 394 were 66 days with antecedent rainfall between 10-15mm, and 1 debris flow event happened;
 395 53 days between 15-20 mm and 4 debris flow events happened; 28 days between 20-25 mm
 396 and 4 debris flow events happened; 30 days between 25-33 mm and 5 debris flow happened;
 397 and 35 days more than 33mm and 9 debris flow events happened. So this group of data can
 398 specifically illustrate the importance of the antecedent rainfall to the debris flow events.



399

400 Figure 10. Rainfall index classifications

401 As Fig. 10 shows, take 1-h rainfall (I_{60}) that obtained from the observed data of the
 402 Guojuanyan gully for the TP. The antecedent precipitation index (API) includes IAP and
 403 DAP, calculated as the following expression (Zhao, 2011; Guo, 2013; Zhuang, 2015):

404
$$API = P_{a0} + R_t \quad (1)$$

405 where P_{a0} is the effective antecedent precipitation (mm) and R_t is the direct antecedent precip-
 406 itation (mm), which is the precipitation from the beginning of the rainfall that trigger debris
 407 flow to the 1 hour before the debris flow.

408 It's difficult to study the influence of antecedent rainfall to debris flow as it mainly relies
 409 on the heterogeneity of soils (strength and permeability properties), which makes it hard to
 410 measure the moisture. Usually, the frequently used method for calculating antecedent daily
 411 rainfall is the weighted sum equation as below (Crozier and Eyles 1980; Glade et al. 2000):

412

$$P_{a0} = \sum_1^n P_i \cdot K_i \quad (2)$$

413

Where P_i is the daily precipitation in the i -th day proceeding to the debris flow event

414

($1 \leq i \leq n$) and K_i is a decay coefficient due to evaporation and geomorphological conditions

415

of the soil. The value of the K , is typically 0.8-0.9, can be determined by the test of soil mois-

416

ture content based on Eq.2 in the watershed. The effect of a rainfall event usually diminishes

417

with the time going forward. Different patterns of storm debris flow gullies require different

418

numbers of previous indirect rainfall days (n), which can be determined by the relationship

419

between the triggering rainfall and the antecedent rainfall of a debris flow (Pan, et al., 2013).

420

If the rainfall is sharp and heavy, the initiation of debris flow would mainly be determined by

421

DAP and TP, while the influence of the antecedent precipitation would be decreased, and vice

422

versa.

423

3.3 The rainfall threshold curve of debris flows

424

3.3.1 The initiation mechanism of hydraulic-driven debris flows

425

When the watershed hydrodynamics, which include the runoff, soil moisture content and

426

the discharge, reach to a certain level, the loose deposits in the channel bed will initiate

427

movement and the sediment concentration of the flow will increase, leading the sediment

428

laden flow to transform into a debris flow. The formation of this kind of debris flow is a com-

429

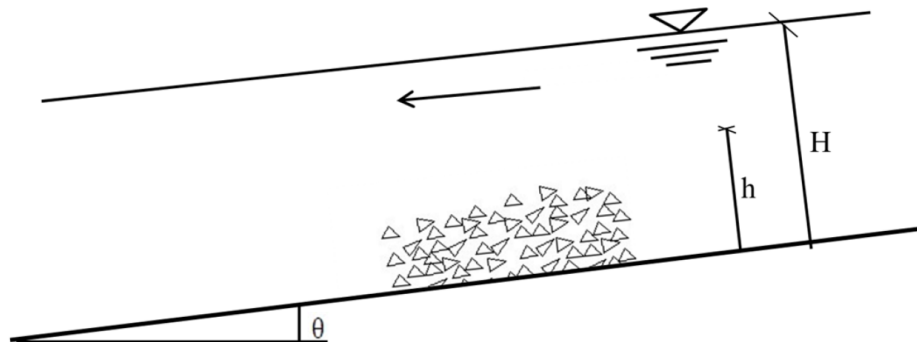
pletely hydrodynamic process. Therefore, it can be regarded as the initiation problem of de-

430

bris flow under hydrodynamic force. The forming process of hydraulic-driven debris flows is

431

shown in Fig. 10.



432

433

Figure 11. The typical debris flow initiate model

434 According to Takahashi's model, the critical depth for hydraulic-driven debris flows is:

$$435 \quad h_0 = \left[\frac{C_*(\sigma - \rho) \tan \phi}{\rho \tan \theta} - \frac{C_*(\sigma - \rho)}{\rho} - 1 \right] d_m \quad (3)$$

436 where C_* is the volume concentration obtained by experiments(0.812); σ is the unit weight of
437 loose deposits (usually is 2.65 g/cm³); ρ is the unit weight of water,1.0 g/cm³; θ is the chan-
438 nel bed slope (°); ϕ is the internal friction angle (°) and can be measured by shear tests ;

439 And d_m is the average grain diameter (mm), which can be expressed as:

$$440 \quad d_m = \frac{d_{16} + d_{50} + d_{84}}{3} \quad (4)$$

441 where d_{16} , d_{50} and d_{84} are characteristic particle sizes of the loose deposits (mm), whose
442 weight percentage are 16%, 50% and 84% separately.

443 Takahashi's model became one of the most common for the initiation of debris flow after
444 it was presented. A great deal of related studies was published based on Takahashi's model
445 later. Some discussed the laws of debris flow according to the geomorphology and the water
446 content (Sassa et al., 2010; Wang, 2016), while others examined the critical conditions of de-
447bris flow with mechanical stability analysis (Cao et al., 2004; Jiang et al., 2017). However,
448 Takahashi's relation was determined for debris flow propagating over a rigid bed, hence, with
449 a minor effect of quasi-static actions near the bed. Lanzoni et al. (2017) slightly modified the
450 Takahashi's formulation of the bulk concentration, which considered the long lasting grain
451 interactions at the boundary between the upper, grain inertial layer and the underlying static
452 sediment bed, and validated the proposed formulation with a wide set of experimental data
453 (Takahashi, 1978, Tsubaki et al., 1983, Lanzoni, 1993, Armanini et al., 2005). The effects of
454 flow rheology on the basis of velocity profiles are analyzed with attention to the role of differ-
455 ent stress-generating mechanisms.

456 This study aims to the initiation of loose solid materials in the gully under surface runoff;
457 the interactions on the boundary are not involved. Therefore, Takahashi's model can be used
458 in this study.

459 **3.3.2 Calculation of watershed runoff yield and concentration**

460 The stored-full runoff, one of the modes of runoff production, is also called as the super

461 storage runoff. The reason of the runoff yeild is that the aeration zone and the saturation zone
 462 of the soil are both saturated. In the humid and semi humid areas where rainfall is plentiful,
 463 because of the high groundwater level and soil moisture content, when the losses of precipita-
 464 tion meet the plant interception and infiltration, it would not increase anymore with the rains
 465 continuous. The Guojuanyan gully is located in Du Jiangyan city, which is in a humid area.
 466 Therefore, stored-full runoff can be used to calculate the watershed runoff. That is, it can be
 467 supposed that the water storage can reach the maximum storage capacity of the watershed in
 468 each heavy rain event. Therefore, the rainfall loss in each time I is the difference between the
 469 maximum water storage capacity I_m and the soil moisture content before the rain P_a . The wa-
 470 ter balance equation of stored-full runoff is expressed as follows (Ye, et al., 1992):

$$471 \quad R = P - I = P - (I_m - P_a) \quad (5)$$

472 where R is the runoff depth (mm); P is the precipitation of one rainfall (mm); I is the rain-
 473 fall loss (mm); I_m is the watershed maximum storage capacity (mm) for a certain watershed,
 474 it is a constant for a certain watershed that can be calculated by the infiltration curve or infil-
 475 tration experiment data. In this study, I_m has been picked up from Handbook of rainstorm
 476 and flood in Sichuan (Sichuan Water and Power Department 1984); and P_a is the antecedent
 477 precipitation index, referring to the total rainfall prior to the 1 hour peak rainfall leading to
 478 debris flow initiation.

479 Eq. 5 can be expressed as follows:

$$480 \quad P + P_a = R + I_m \quad (6)$$

481 The precipitation intensity is a measure of the peak precipitation. At the same time, the
 482 duration of the peak precipitation is generally brief, lasting only up to tens of minutes. There-
 483 fore, 10-minute precipitation intensity (maximum precipitation over a 10-minute period dur-
 484 ing the rainfall event) is selected as the triggering rainfall for debris flow, which is appropriate
 485 and most representative. However, it is difficult to obtain such short-duration rainfall data in
 486 areas with scarcity of data. Therefore, in this study, P and P_a are replaced by I_{60} (1 hour
 487 rainfall) and API (the antecedent precipitation index), respectively; thus, Eq. 6 is expressed
 488 as:

$$489 \quad I_{60} + API = R + I_m \quad (7)$$

490 In the hydrological study, the runoff depth R is:

$$491 \quad R = \frac{W}{1000F} = \frac{3.6 \sum Q \cdot \Delta t}{F} = \frac{3.6Q}{F} \quad (8)$$

492 where R is the runoff depth (m); W is the total volume of runoff (m³); F is the watershed area
493 (km²); Δt is the duration time, in this study it is 1 hour; and Q is the average flow of the water-
494 shed (m³/s), which can be expressed as follows:

$$495 \quad Q = BVh_0 \quad (9)$$

496 where B is the width of the channel (m), V is the average velocity (m/s) and h_0 is the critical
497 depth (m).

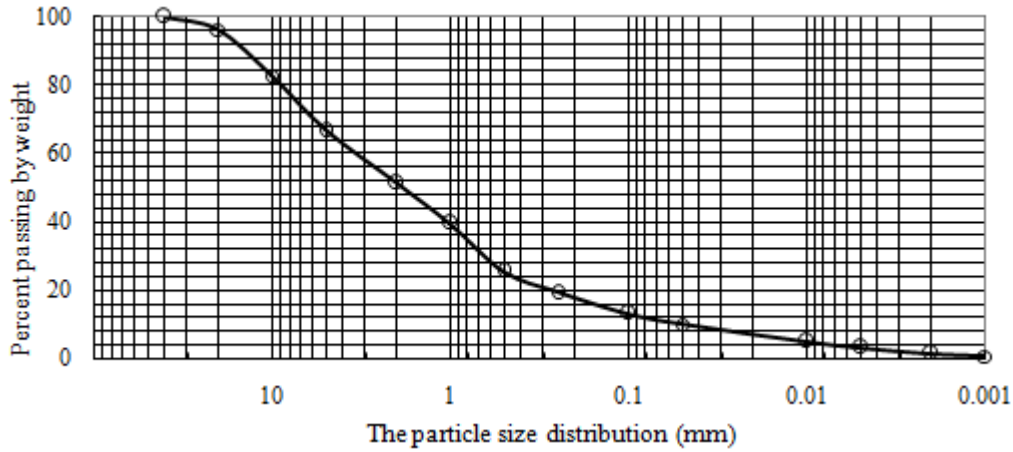
498 Eq. 7 is the expression of the rainfall threshold curve for a watershed, which can be used
499 for debris flow early warning. This proposed rainfall threshold curve is a function of the ante-
500 cedent precipitation index (API) and 1 hour rainfall (I_{60}), which is a line and a negative
501 slope.

502 **4 Results**

503 **4.1 The rainfall threshold curve of debris flow**

504 **4.1.1 The critical depth of the Guojuanyan gully**

505 The grain grading graph (Fig. 11) is obtained by laboratory grain size analysis experi-
506 ments for the loose deposits of the Guojuanyan gully. Figure 11 shows that the characteristic
507 particle sizes d_{16} , d_{50} , d_{84} and d_m are 0.18 mm, 1.9 mm, and 10.2 mm, 4.1 mm, respective-
508 ly. According to Eq. (1), the critical depth (h_0) of the Guojuanyan gully is 7.04 mm.



509
510

Figure 11. The grain grading graph of the Guojuanyan gully

511 **Table 4.** Critical water depth of debris flow triggering in Guojuanyan gully

C_*	σ (g/cm ³)	ρ (g/cm ³)	$\tan \theta$	d_{16} (mm)	d_{50} (mm)	d_{84} (mm)	d_m (mm)	ϕ (°)	$\tan \phi$	h_0 (mm)
0.812	2.67	1.0	0.333	0.18	1.9	10.2	4.1	21.21	0.388	7.04

512 4.1.2 The rainfall threshold curve of debris flow

513 Taking the cross-section at the outlet of the debris flow formation region as the computa-
514 tion object, based on the field investigations and measurements, the width of the cross-section
515 is 20 m, and the average velocity of debris flows which is calculated by the several debris flow
516 events, is 1.5m/s. Based on the Handbook of rainstorm and flood in Sichuan (Sichuan Water
517 and Power Department 1984), the watershed maximum storage capacity (I_m) of the
518 Guojuanyan gully is 100mm. According to Eq. (5) - Eq. (7), the calculated rainfall threshold
519 curve of debris flow in the Guojuanyan gully is shown in Table 5.

520 **Table 5.** The calculated process of the rainfall threshold

Watershed	h_0 (mm)	B (m)	V (m/s)	Q (m ³ /s)	Δt (h)	F (km ²)	R (mm)	I_m (mm)	$R + I_m$ (mm)
Guojuanyan	7.04	20.0	1.5	0.197	1	0.11	6.9	100	106.9

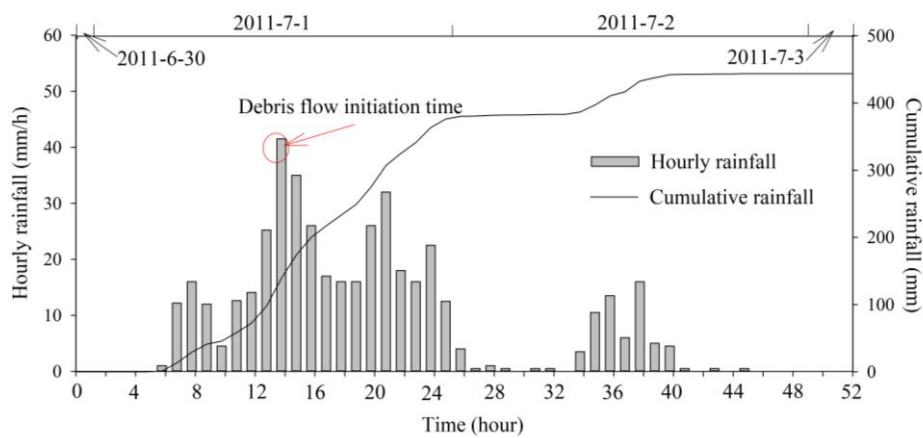
521 From the calculated results, we can conclude the rainfall threshold of the debris flow is
522 $I_{60} + API = R + I_m = 106.9 \approx 107$ mm; that is, when the sum of the antecedent precipitation in-
523 dex (API) and the 1 hour rainfall (I_{60}) reaches 107 mm (early warning area), the gully may

524 trigger debris flow.

525 4.2 Validation of the results

526 4.2.1 The typical debris flow events in the Guojuanyan gully after earthquake

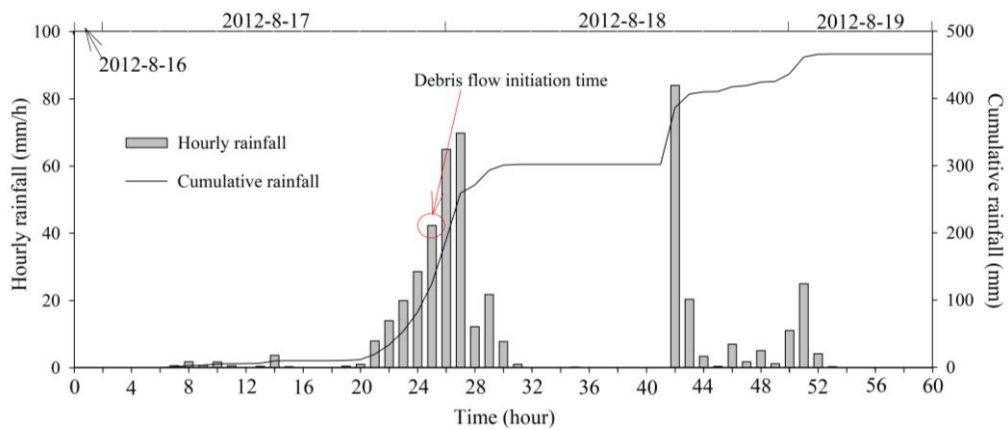
527 Five typical debris flow events and the corresponding rainfall processes are showed in
528 Figure 13. The debris flow initiation time and the rainfall, both hourly rainfall and cumulative
529 rainfall, have been recorded. From Fig.13, the five debris flows were triggered by torrential
530 rains.



531

(a)

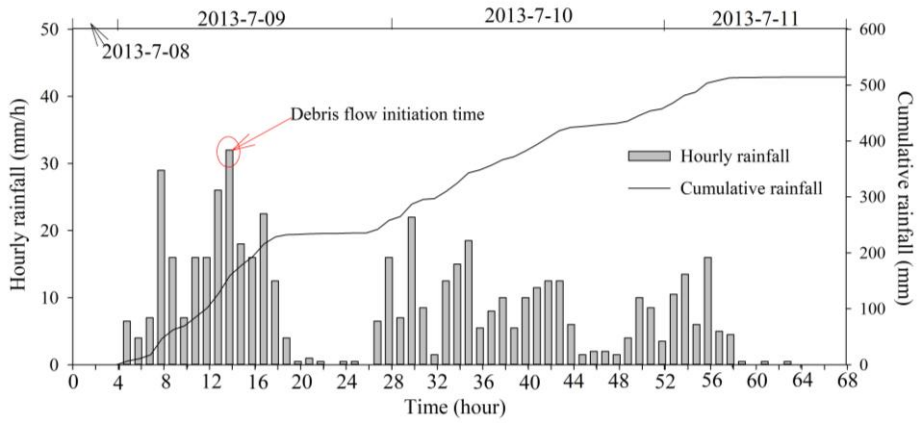
532



533

(b)

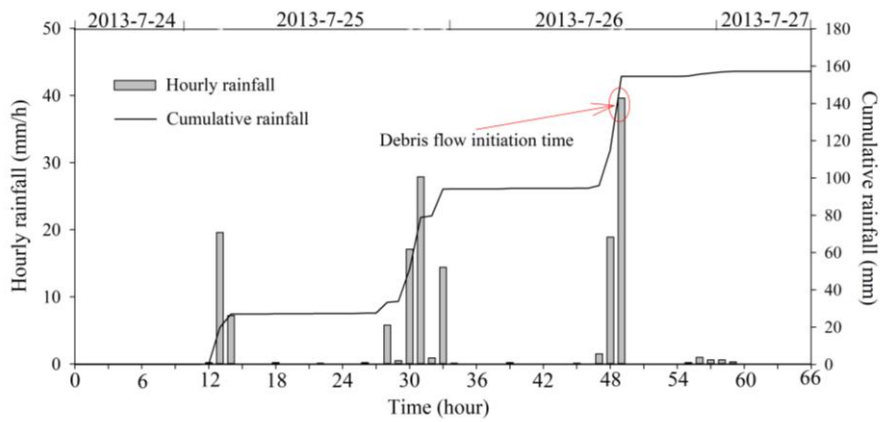
534



535

536

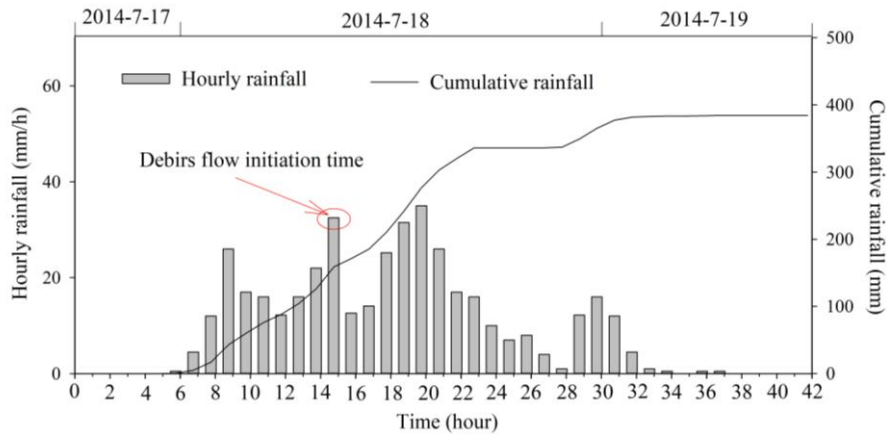
(c)



537

538

(d)



539

540

(e)

541 **Figure 13.** The rainfall process of debris flow events in the Guojuanyan gully from 2011 to 2014 (a, July
 542 1, 2011; b, August 17, 2012; c, July 9, 2013; d, July 26, 2013; e, July 18, 2014)

543 **4.2.2 The calculation of API and 1-h triggering rainfall of the typical rain-**
 544 **storms during 2010-2014**

545 Based on the field tests and experiences, the value of K in Eq.2 is identified as 0.8 (Cui et
546 al. 2007). To determine the numbers of previous indirect rainfall days (n), a comparison
547 among 3 days, 10days, 20days and 30 days were showed in Table 6. It indicates that the val-
548 ue of the effective antecedent precipitations (P_{a0}) were increasing from 3 days to 20 days,
549 while with the time last to 30 days, the value of P_{a0} was barely changed. Therefore, it can be
550 considered that the effect of a rainfall event usually diminished in 20 days. Hence, the num-
551 bers of previous indirect rainfall days (n) is identified as 20.

552 **Table 6.** The comparisons of P_{a0} when n have different values

Time	$P_{a0}(\text{mm})$			
	n=3	n=10	n=20	n=30
July 1, 2011	3.4	5.2	9.7	9.7
August 17, 2012	2.3	4.7	12.1	12.1
July 9, 2013	0.8	2.5	5.7	5.7
July 26, 2013	6.2	10.8	22.4	22.6
July 18, 2014	0	6.2	10.7	10.7
August 20, 2011	8.3	0	8.5	8.6
September 5, 2011	21.3	45.9	48.7	48.8
June 16, 2012	0	2.7	5.6	5.6
August 3, 2012	5.6	6.1	7.5	7.5
August 18, 2012	10.2	18.4	54.3	54.3
June 18, 2013	0	2.8	6.2	6.2
July 28, 2013	0.2	1.7	13.4	13.5
August 6, 2013	0.2	6.6	12.4	12.4

553

554 Thus, the intensity of the 1-h triggering rainfall I_{60} and cumulative rainfall for the typi-
555 cal rainstorms are shown in Table 7. In addition to the rainfall process of the 5 debris flow
556 events (Fig. 13), some typical rainfalls whose daily rainfall were greater than 50 mm but did
557 not trigger a debris flow were also calculated as a contrast; the greatest 1-h rainfall is consid-
558 ered as I_{60} .

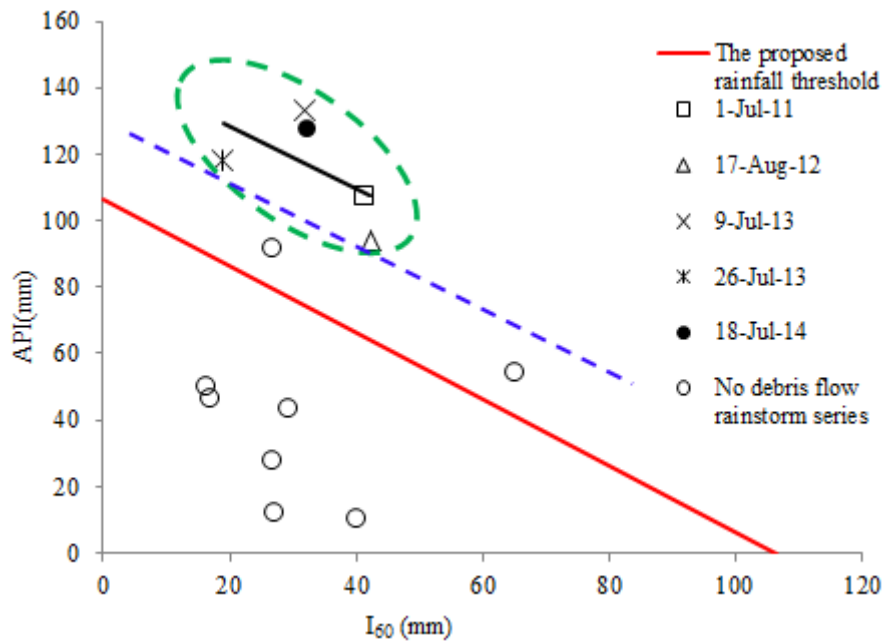
559 **Table 7.** The data of typical rainfall in the Guojuanyan gully after the earthquake

Time	Daily rainfall (mm)	P_{a0} (mm)	R_t (mm)	API (mm)	I_{60} (mm)	$API+I_{60}$ (mm)	Location to the threshold line	Triggered debris flow
1 July, 2011		9.7	97.6	107.3	41.5	148.8	Above	Yes
17 August , 2012		12.1	81.9	94.0	42.3	136.3	Above	Yes
9 July , 2013		5.7	127.5	133.2	32	165.2	Above	Yes
26 July , 2013		22.4	96.0	118.4	18.9	137.3	Above	Yes
18 July, 2014		10.7	116.2	126.9	32.5	159.4	Above	Yes
20 August , 2011	82.8	8.5	19.0	27.5	26.8	54.3	Below	No
5 September , 2011	52.1	48.7	1.2	49.9	16.2	66.1	Below	No

16 June , 2012	55.8	5.6	6.6	12.2	27.0	39.2	Below	No
3 August , 2012	148.3	7.5	84.3	91.8	26.7	118.5	Above	No
18 August , 2012	125.7	54.3	0	54.3	65.0	119.3	Above	No
18 June , 2013	50.6	6.2	3.8	10.0	40.0	50.0	Below	No
28 July , 2013	59.4	13.4	30.0	43.4	29.4	72.8	Below	No
6 August , 2013	56.1	12.4	34.0	46.4	17.1	63.5	Below	No

560

561 The proposed rainfall threshold curve is shown in Figure 14, in which the red real line de-
562 fines the threshold relationship. It shows that the calculated values $I_{60} + API$ of debris flow
563 events in the Guojuanyan gully are all above the rainfall threshold curve, while most of the
564 rainstorms that did not trigger debris flow are lay below the curve. Therefore, it indicates that
565 the rainfall threshold curve calculated by this work is reasonable through the validation by
566 rainfall and hazards data of the Guojuanyan gully.



567

568 **Figure 14.** The calculated rainfall threshold curve (red real line), the trend line (black real line) of the
569 debris flow events and the debris flows triggering thresholds (dashed line) in Guojuanyan gully

570 5 Discussions

571 The trend of the debris flow events as well as the debris flow thresholds were analyzed in
572 Fig. 14 by using the monitoring rainfall data. A comparison between the thresholds and the
573 calculated threshold curve indicates that they have the same laws. Therefore, the threshold
574 calculated method proposed in this work is reasonable and can be used in the areas with scar-
575 city of data. The proposed rainfall threshold curve is a function of the antecedent precipita-

576 tion index (API) and the 1-h rainfall (I_{60}), which has been validated by rainfall and hazards
577 data. It should be noted that the proposed approach is based on a procedure that can be ex-
578 ported elsewhere only if a site-specific calibration is needed to develop specific thresholds for
579 other test sites. Therefore, the specific value of the threshold should be calculated by the initi-
580 ation conditions of the debris flow in specific gully.

581 However, this work still has two limitations. In Figure 14, there are two points above the
582 curve that did not trigger debris flow at all. Although we have highlighted the significance and
583 interconnect of antecedent rainfall, critical rainfall, 1-h triggering rainfall, as well as their ac-
584 curate determination before the hour of debris flow triggering, it should be noticed that the
585 rainfall is only the triggering factor of debris flows. A comprehensive warning system must
586 contain more environmental factors, such as the geologic and geomorphologic factors, the
587 distribution of material source. In addition, the special and complex formative environment of
588 debris flow after earthquake caused the rainfall threshold is much more complex and uncer-
589 tain. The rainfall threshold of debris flow is influenced by the antecedent precipitation index
590 (API), rainfall characteristics, amount of loose deposits, channel and slope characteristics,
591 and so on. Therefore, we should further study the characteristics of the movable solid materi-
592 als, the shape of gully, and so on to modify the rainfall threshold curve. But, on the other
593 hand, if given the two rainstorms under the threshold, all the debris flow events points will
594 still locate above the threshold and there will have no missed alarms. Therefore, the threshold
595 established in this work is a conservative one and respect safety.

596 On the other hand, restricted by the limited rainfall data, this study was validated by only
597 5 debris flow events. Another limitation of this work is that the approach proposed in this
598 study hasn't been validated by other gullies except the Guojuanyan gully so far. Figure 13 and
599 Figure 14 indicated that the only 5 debris flow events all triggered by the rainfalls with
600 high-intensity and short-duration. In the future, the value of the curve should be further vali-
601 dated and continuously corrected with more rainfall and disaster data in later years.

602 **6 Conclusions**

603 (1) In the Wenchuan earthquake affected areas, loose deposits are widely distributed,
604 causing dramatic changes on the environmental development for the occurrence of debris
605 flow; thus, the debris flow occurrence increased dramatically in the subsequent years. The

606 characteristics of the 10-min, 1-h and 24-h critical rainfalls were represented based on a com-
607 prehensive analysis of limited rainfall and hazards data. The statistical results show that the
608 10-min and 1-h critical rainfalls of different debris flow events have minor differences; how-
609 ever, the 24 hour critical rainfalls vary widely. The 10-min and 1-h critical rainfalls have a no-
610 tably higher correlation with debris flow occurrences than to the 24-h critical rainfalls.

611 (2) The rainfall pattern of the Guojuanyan gully is the peak pattern, both single peak and
612 multi-peak. The antecedent precipitation index (*API*) was fully explored by the antecedent
613 effective rainfall and triggering rainfall.

614 (3) As an important and effective means of debris flow early warning and mitigation, the
615 rainfall threshold of debris flow was determined in this paper, and a new method to calculate
616 the rainfall threshold is put forward. Firstly, the rainfall characteristics, hydrological charac-
617 teristics, and some other topography conditions were analyzed. Then, the critical water depth
618 for the initiation of debris flows is calculated according to the topography conditions and
619 physical characteristics of the loose solid materials. Finally, according to the initiation mecha-
620 nism of hydraulic-driven debris flow, combined with the runoff yield and concentration laws
621 of the watershed, this study promoted a new method to calculate the debris flow rainfall
622 threshold. At last, the hydrological condition for the initiation of a debris flow is the result of
623 both short-duration heavy rains (I_{60}) and the antecedent precipitation index (*API*). The
624 proposed approach resolves the problem of debris flow early warning in areas with scarcity
625 data, can be used to establish warning systems of debris flows for similar catchments in areas
626 with scarcity data although it still need further modification. This study provides a new
627 thinking for the debris flow early warning in the mountain areas.

628 **Acknowledgments**

629 This paper is supported by the CRSRI Open Research Program (Program No:
630 CKWV2015229/KY), National Key R&D Program of China (2017YFC1502502), CAS Pioneer
631 Hundred Talents Program, and National Nature Science Foundation of China (No. 41372331 ,
632 No. 41672318 & No.51679229).

633 **References**

634 Althuwaynee OF, Pradhan B, Ahmad N (2015) Estimation of rainfall threshold and its use in landslide hazard
635 mapping of Kuala Lumpur metropolitan and surrounding areas. *Landslides* 12:861-875.
636 doi:10.1007/s10346-014-0512-y

637 Bai LP, Sun JL, Nan Y (2008) Analysis of the critical rainfall thresholds for mudflow in Beijing, China. *Geological*
638 *Bulletin of China* 27(5): 674-680. (in Chinese)

639 Baum RL, Godt JW (2010). Early warning of rainfall-induced shallow landslides and debris flows in the USA.
640 *Landslides*, 7(3):259–272.

641 Bogaard, T. and Greco, R. (2018) Invited perspectives: Hydrological perspectives on precipitation intensity-duration
642 thresholds for landslide initiation: proposing hydro-meteorological thresholds, *Nat. Hazards Earth Syst. Sci.*, 18,
643 31–39, <https://doi.org/10.5194/nhess-18-31-2018>

644 Caine, N (1980) The rainfall intensity-duration control of shallow landslides and debris flows. *Physical Geography*
645 62A (1-2):23-27

646 Campbell RH (1975) Debris Flow Originating from Soil Slip during Rainstorm in Southern California. *Q. Engineering*
647 *Geologist*7: 339–349. DOI:10.1144/GSL.QJEG.1974.007.04.04

648 Canli, E., Mergili, M., and Glade, T. (2017) Probabilistic landslide ensemble prediction systems: Lessons to be learned
649 from hydrology, *Nat. Hazards Earth Syst. Sci. Discuss.*, <https://doi.org/10.5194/nhess-2017-427>, in review

650 Cannon, Susan H., et al. (2008) Storm rainfall conditions for floods and debris flows from recently burned areas in
651 southwestern Colorado and southern California. *Geomorphology* 96(3): 250-269.

652 Cao Z., Pender G., Wallis S., Carling P. (2004) Computational dam-break hydraulics over erodible sediment bed.
653 *Journal of hydraulic engineering* 130.7 (2004): 689-703.

654 Chen, Su-Chin, and Bo-Tsung Huang (2010) Non-structural mitigation programs for sediment-related disasters after
655 the Chichi Earthquake in Taiwan. *Journal of Mountain Science* 7(3): 291-300.

656 Chen YS (2008) An influence of earthquake on the occurrence of landslide and debris flow. Taipei: National Cheng
657 Kung University.

658 Chen YJ, Yu B, Zhu Y, et al. (2013) Characteristics of critical rainfall of debris flow after earthquake - a case study of
659 the Xiaogangjian gully. *Journal of Mountain Science* 31(3): 356-361. (in Chinese)

660 Cheng ZL, Zhu PY, Liu LJ (1998) The Relationship between Debris Flow Activity and Rainfall Intensity. *Journal of*
661 *Natural Disasters*7 (1): 118–120. (in Chinese)

662 Chen NS, Yang CL, Zhou W, et al. (2009) The Critical Rainfall Characteristics for Torrents and Debris Flows in the
663 Wenchuan Earthquake Stricken Area. *Journal of Mountain Science* 6: 362-372. DOI: 10.1007/s11629-009-1064-9

664 Cui P (1991) Experiment Research of the Initial Condition and Mechanism of Debris Flow. *Chinese Science Bulletin*
665 21:1650–1652. (in Chinese)

666 Cui P, Hu KH, Zhuang JQ, Yang Y, Zhang J (2011) Prediction of debris-flow danger area by combining hydro-logical
667 and inundation simulation methods. *Journal of Mountain Science* 8(1): 1-9. doi: 10.1007/s11629-011-2040-8

668 Cui P, Zhu YY, Chen J, et al. (2007) Relationships between antecedent rainfall and debris flows in Jiangjia Ravine,
669 China. In: Chen C L and Majir JJ (eds.), *Debris flow hazard mitigation mechanics, Prediction, and Assessment*.
670 Millpress, Rotterdam: 1-10.

671 Dahal RK, Hasegawa S, Nonomura A, et al. (2009) Failure characteristics of rainfall-induced shallow landslides in

672 granitic terrains of Shikoku Island of Japan. *Environmental geology* 56(7): 1295-1310. DOI:
673 10.1007/s00254-008-1228-x

674 Degetto M, Gregoretti C, Bernard M (2015) Comparative analysis of the differences between using LiDAR
675 contour-based DEMs for hydrological modeling of runoff generating debris flows in the Dolomites. *Front. Earth Sci.*
676 3, 21. doi: 10.3389/feart.2015.00021

677 **Frattini P, Crosta G, Sosio R (2009) Approaches for defining thresholds and return periods for rainfall - triggered**
678 **shallow landslides. *Hydrol Proc* 23(10):1444-1460. doi:10.1002/hyp.7269**

679 Gregoretti C, Degetto M, Boreggio M (2016) GIS-based cell model for simulating debris flow runout on a fan. *Journal*
680 *of Hydrology* 534: 326-340. doi: 10.1016/j.jhydrol.2015.12.054

681 Guido Rianna, Luca Pagano, Gianfranco Urciuoli (2014) Rainfall patterns triggering shallow flowslides in pyroclastic
682 soils. *Engineering Geology*, 174: 22-35 doi: 10.1016/j.enggeo.2014.03.004

683 Guo, X.J., Cui, P., Li, Y., 2013. Debris flow warning threshold based on antecedent rainfall: a case study in Jiangjia
684 Ravine, Yunnan, China. *J. Mt. Sci.* 10 (2), 305–314.

685 Guzzetti, F., Peruccacci, S., Rossi, M., & Stark, C. P. (2008). The rainfall intensity–duration control of shallow
686 landslides and debris flows: an update. *Landslides*, 5(1), 3-17.

687 Hu M J, Wang R (2003) Testing Study of the Correlation among Landslide, Debris Flow and Rainfall in Jiangjia Gully.
688 *Chinese Journal of Rock Mechanics and Engineering*, 22(5): 824–828 (in Chinese)

689 Hong Y, Hiura H, Shino K, et al. (2005) The influence of intense rainfall on the activity of large-scale crystalline schist
690 landslides in Shikoku Island, Japan. *Landslides* 2(2): 97-105. DOI: 10.1007/s10346-004-0043-z

691 Hu W, Dong XJ, Wang GH, van Asch TWJ, Hicher PY (2016) Initiation processes for run-off generated debris flows
692 in the Wenchuan earthquake area of China. *Geomorphology* 253: 468–477. doi: 10.1016/j.geomorph.2015.10.024

693 Iverson RM, Lahusen RG (1989) Dynamic Pore-Pressure Fluctuations in Rapidly Shearing Granular Materials.
694 *Science* 246 (4931): 796–799. DOI: 10.1126/science.246.4931.796

695 Jianqi Zhuang, Peng Cui, Gonghui Wang, et al. (2015) Rainfall thresholds for the occurrence of debris flows in the
696 Jiangjia Gully, Yunnan Province, China. *Engineering Geology*, 195: 335-346.

697 **Jiang X., Cui P., Chen H., Guo Y. (2016) Formation conditions of outburst debris flow triggered by overtopped natural**
698 **dam failure. *Landslides* 14(3):1-11.**

699 Jibson RW (1989) Debris flows in southern Puerto Rico. *Geological Society of America Special Papers* 236: 29-56.
700 DOI: 10.1130/SPE236-p29

701 Jun Wang, Shun Yang, Guoqiang Ou, et al. (2017) Debris flow hazards assessment by combining numerical simulation
702 and land utilization. *Bulletin of Engineering Geology and the Environment*, 1-15. Doi: 10.1007/s10064-017-1006-7

703 **Lagomarsino D, Segoni S, Rosi A, Rossi G, Battistini A, Catani F, Casagli N (2015) Quantitative comparison between**
704 **two different methodologies to define rainfall thresholds for landslide forecasting. *Nat Hazards Earth Syst Sci***
705 **15:2413–2423. doi:10.5194/nhess-15-2413-2015**

706 Liang GM, Yao LK (2008) Study on the critical rainfall for debris flows. *Lu Ji Gongcheng* 6: 3-5. (in Chinese)

707 Liu YH, Tang C, Li TF, et al. (2009) Statistical relations between geo-hazards and rain type. *Journal of Engineering*
708 *Geology* 17(5): 656-661. (in Chinese)

709 Liu JF, You Y, Chen XZ, Fan JR (2010) Identification of potential sites of debris flows in the upper Min River
710 drainage, following environmental changes caused by the Wenchuan earthquake. *Journal of Mountain Science* 3:
711 255-263. doi: 10.1007/s11629-010-2017-z

712 Lanzoni, S., C. Gregoretti, and L. M. Stancanelli (2017) Coarse-grained debris flow dynamics on erodible beds, *J. Ge-*
713 *ophys. Res. Earth Surf.*, 122, doi:10.1002/2016JF004046.

714 McCoy SW, Kean JW, Coe JA, Tucker GE, Staley DM, Wasklewicz WA (2012) Sediment entrainment by debris flows:
715 In situ measurements from the head waters of a steep catchment. *J. Geophys. Res.*117, F03016. doi:
716 10.1029/2011JF002278

717 Mohamad Ayob Mohamadi, Ataollah Kavian (2015) Effects of rainfall patterns on runoff and soil erosion in field plots.
718 *International Soil and Water Conservation Research* 3: 273-281.
719 <http://dx.doi.org/10.1016/j.iswcr.2015.10.001>Imaizumi F, Sidle RC, Tsuchiya S, Ohsaka O (2006)
720 Hydrogeomorphic processes in a steep debris flow initiation zone. *Geophys. Res. Lett.* 33, L10404. doi:
721 10.1029/2006GL026250

722 Pan HL, Ou GQ, Hang JC, et al.(2012)Study of rainfall threshold of debris flow forewarning in data lack areas. *Rock*
723 *and Soil Mechanics* 33(7): 2122-2126. (in Chinese)

724 Pan HL, Huang JC, Wang R, et al. (2013) Rainfall Threshold Calculation Method for Debris FlowPre-Warning in
725 Data-Poor Areas. *Journal of Earth Science* 24(5): 854–862. DOI:10.1007/s12583-013-0377-3

726 Rosi A, Lagomarsino D, Rossi G, Segoni S, Battistini A, Casagli N (2015) Updating EWS rainfall thresholds for the
727 triggering of landslides. *Nature Hazard* 78:297–308

728 Saito H, Nakayama D, Matsuyama H (2010) Relationship between the initiation of a shallow landslide and rainfall
729 intensity—duration thresholds in Japan. *Geomorphology* 118(1): 167-175. DOI: 10.1016/j.geomorph.2009.12.016

730 Sassa, K., Nagai, O., Solidum, R., Yamazaki, Y., & Ohta, H. (2010) An integrated model simulating the initiation and
731 motion of earthquake and rain induced rapid landslides and its application to the 2006 Leyte landslide. *Landslides*,
732 7(3), 219-236.

733 Segoni S, Battistini A, Rossi G, Rosi A, Lagomarsino D, Catani F, Moretti S, Casagli N (2015) Technical note: an
734 operational landslide early warning system at regional scale based on space–time variable rainfall thresholds. *Nat*
735 *Hazards Earth Syst Sci* 15: 853–861

736 Segoni S, Rosi A, Lagomarsino D, Fanti R, and Casagli N (2018) Brief Communication: Using averaged soil moisture
737 estimates to improve the performances of a regional-scale landslide early warning system. *Nat. Hazards Earth Syst.*
738 *Sci.*

739 Shied CL, Chen LZ (1995) Developing the critical line of debris –flow occurrence. *Journal of Chinese Soil and Water*
740 *Conservation* 26(3):167-172. (in Chinese)

741 Shieh CL, Chen YS, Tsai YJ, et al (2009) Variability in rainfall threshold for debris flow after the Chi-Chi earthquake
742 in central Taiwan, China. *International Journal of Sediment Research* 24(2): 177-188.

743 Staley, D.M., Kean, J.W., Cannon, S.C., Schmidt, K.M., Laber, J.L. (2013) Objective definition of rainfall
744 intensity–duration thresholds for the initiation of post-fire debris flows in southern California, *Landslides* 10,
745 547–562

746 Takahashi T (1978) Mechanical Characteristics of Debris Flow. *Journal of the Hydraulics Division* 104:1153–1169

747 Tang C, Zhu J, Li WL (2009) Rainfall-triggered debris flows following the Wenchuan earthquake. Bull Eng Geol
748 Environ 68(2):187–194. DOI: 10.1007/s10064-009-0201-6

749 Tang C, Van Asch TWJ, Chang M, et al.(2012)Catastrophic debris flows on 13 August 2010 in the Qingping area,
750 southwestern China: the combined effects of as trong earthquake and subsequent rainstorms.
751 Geomorphology139–140:559–576. DOI: 10.1016/j.geomorph.2011.12.021

752 Tang C, Zhu J, Chang M, et al. (2012) An empirical–statistical model for predicting debris-flow runout zones in the
753 Wenchuan earthquake area. Quaternary International 250:63–73. DOI:10.1016/j.quaint.2010.11.020.

754 Tecca PR, Genevois R (2009) Field observations of the June 30, 2001 debris flow at Acquabona (Dolomites, Italy).
755 Landslides 6(1): 39-45. doi: 10.1007/s10346-009-0145-8

756 Tian B, Wang YY, Hong Y (2008) Weighted relation between antecedent rainfall and processprecipitation in debris
757 flow prediction—A case study ofJiangjia gully in Yunnan province. Bulletin of Soil and Water Conservation28(2):
758 71-75.(in Chinese)

759 Tiranti D, Deangeli C (2015) Modeling of debris flow depositional patterns according to the catchment and sediment
760 source area characteristics. Front. Earth Sci. 3, 8. doi: 10.3389/feart.2015.00008

761 Tofani et al., Soil characterization for shallow landslides modeling: a case study in the Northern Apennines (Central
762 Italy). 2017. Landslides 14:755–770, DOI 10.1007/s10346-017-0809-8

763 Y.Zhao, F. Wei, H.Yang, et al. (2011) Discussion on Using Antecedent Precipitation Index to Supplement Relative Soil
764 Moisture Data Series. Procedia Environment Sciences 10: 1489-1495.

765 Wang EC, Meng QR (2009) Mesozoic and cenozoic tectonic evolution of the Longmenshan fault belt. Science in China
766 Series D: Earth Sciences 52(5): 579-592. DOI:10.1007/s11430-009-0053-8

767 Wang G., Furuya G., Zhang F., Doi I., Watanabe N. (2016) Layered internal structure and breaching risk assessment
768 of the Higashi-Takezawa landslide dam in Niigata, Japan. Geomorphology, 267:48-58.

769 Wang J, Ou GQ, Yang S, Lu GH, et al. (2013) Applicability of geomorphic information entropy in the post-earthquake
770 debris flow risk assessment. Journal of Mountain Science 31(1): 83-91. (in Chinese)

771 Wang J, Yu Y, Yang S, et al.(2014) A Modified Certainty Coefficient Method (M-CF) for Debris Flow Susceptibility
772 Assessment: A Case Study for the Wenchuan Earthquake Meizoseismal Areas. Journal of Mountain Science11(5):
773 1286-1297. DOI: 10.1007/s11629-013-2781-7.

774 Wang J, Yu Y, Ou GQ, et al.(2016) Study on the Geotechnical Mechanical Characteristics of Loose Materials in the
775 Wenchuan Earthquake-hit Areas. Science Technology and Engineering 16(5): 11-18. (in Chinese)

776 Wieczorek GF (1987) Effect of rainfall intensity and during in debris flows in central Santa Cruz Mountain. California.
777 Engineering Geology 7: 93-104. DOI: 10.1130/REG7-p93

778 Wilson, RC, Jayko AS (1997) Preliminary Maps ShowingRainfall Thresholds for Debris-Flow Activity, San
779 Franciscoby Region, California. U.S. Geological SurveyOpen-File Report 97-745 F

780 Winter, M. G., et al. (2010) Debris flow, rainfall and climate change in Scotland. Quarterly Journal of Engineering
781 Geology and Hydrogeology 43(4): 429-446.

782 Xu ZQ, Ji SC, Li HB, et al. (2008)Uplift of the Longmen Shan range and the Wenchuan earthquake. Episodes 31(3):
783 291-301

784 Xu Q, Zhang S, Li WL, et al.(2012) The 13 August 2010catastrophic debris flows after the 2008 Wenchuan earthquake,

785 China. *Natural hazards and earth system sciences* 12(1):201–216. DOI: 10.5194/nhess-12-201-2012

786 Yao LK (1988) A research on the calculation of critical rainfall with frequency of debris flow and torrential rain.

787 *Journal of Soil and Water Conservation* 2(4): 72-78 (in Chinese)

788 Ye SZ (1992) *Hydrological calculation*. Water conservancy and Hydropower Press, 111.

789 Zhou, W., & Tang, C. (2014). Rainfall thresholds for debris flow initiation in the Wenchuan earthquake-stricken area,

790 southwestern China. *Landslides*, 11(5), 877-887.

791 Zhuang JQ, Cui P, Ge YG, et al. (2009) Relationship between rainfall characteristics and total amount of debris flow.

792 *Journal of Beijing Forestry University* 31(4): 77-83 (in Chinese)

793 Zhang SJ, Yang HJ, Wei FQ, et al. (2014) A Model of Debris Flow Forecast Based on the Water-Soil Coupling

794 Mechanism. *Journal of Earth Science*, 25(4): 757-763. DOI:10.1007/s12583-014-0463-1

795 Zhenlei Wei, Yuequan Shang, Yu Zhao, et al. (2017) Rainfall threshold for initiation of channelized debris flows in a

796 small catchment based on in-site measurement. *Engineering Geology*, 217, 23-34.